Article

Cell Reports

Synaptic Remodeling Depends on Signaling between Serotonin Receptors and the Extracellular Matrix

Graphical Abstract

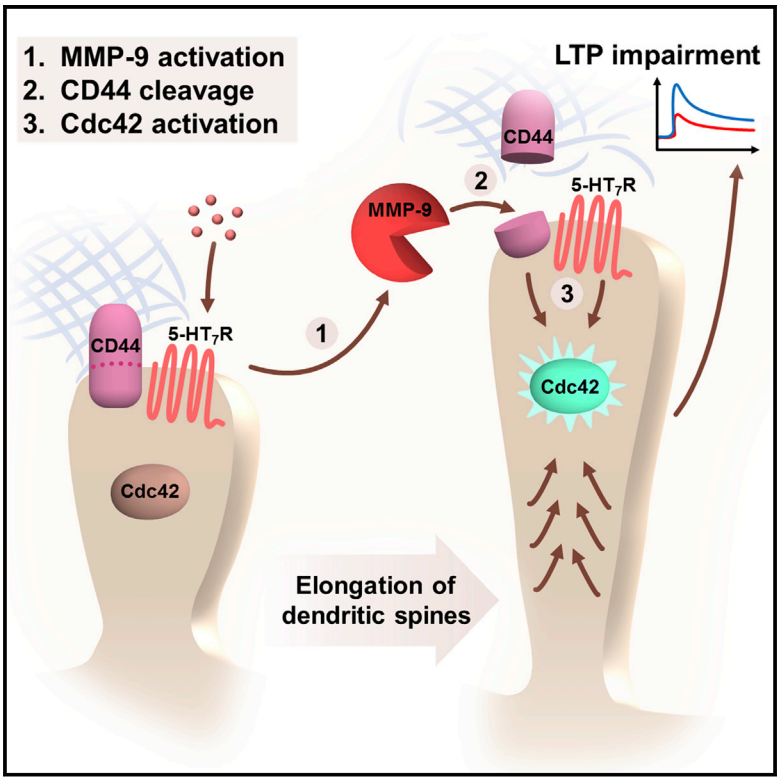

Authors

Monika Bijata, Josephine Labus, Daria Guseva, ..., Grzegorz Wilczyński, Jakub Wlodarczyk, Evgeni Ponimaskin

Correspondence

j.wlodarczyk@nencki.gov.pl (J.W.), ponimaskin.evgeni@mh-hannover.de (E.P.)

In Brief

Bijata et al. examine a signaling module involving the 5-HT7 receptor (5-HT7R), matrix metalloproteinase 9 (MMP-9), the hyaluronan receptor CD44, and the small GTPase Cdc42. Stimulation of 5-HT7R results in MMP-9 activation, which, in turn, cleaves CD44. This results in local detachment from the ECM, thus facilitating spine elongation via 5-HT7R/Cdc42 signaling.

Highlights

- The 5-HT7 receptor, MMP-9, CD44, and the small GTPase Cdc42 belong to the same signaling module
- 5-HT7R and CD44 form a protein complex in the brain
- CD44 is a substrate for MMP-9 cleavage in neurons
- 5-HT7R stimulation increases MMP-9 activity, triggering dendritic spine remodeling

Bijata et al., 2017, Cell Reports *19*, 1767–1782
May 30, 2017
http://dx.doi.org/10.1016/j.celrep.2017.05.023

CellPress

Cell Reports
Article

Synaptic Remodeling Depends on Signaling between Serotonin Receptors and the Extracellular Matrix

Monika Bijata,[1] Josephine Labus,[2] Daria Guseva,[2] Michał Stawarski,[1] Malte Butzlaff,[2] Joanna Dzwonek,[3] Jenny Schneeberg,[4,5] Katrin Böhm,[4,5] Piotr Michaluk,[1,6] Dmitri A. Rusakov,[6] Alexander Dityatev,[4,5] Grzegorz Wilczyński,[3] Jakub Wlodarczyk,[1,*] and Evgeni Ponimaskin[2,7,*]

[1]Department of Molecular and Cellular Neurobiology, Nencki Institute of Experimental Biology of the Polish Academy of Science, Pasteura 3, Warsaw 02-093, Poland

[2]Cellular Neurophysiology, Center of Physiology, Hannover Medical School, Carl-Neuberg-Str. 1, 30625 Hannover, Germany

[3]Department of Neurophysiology, Nencki Institute of Experimental Biology of the Polish Academy of Science, Pasteura 3, Warsaw 02-093, Poland

[4]Molecular Neuroplasticity Group, German Center for Neurodegenerative Diseases (DZNE), Leipziger Str. 44, 39120 Magdeburg, Germany

[5]Medical Faculty, Otto von Guericke University, Leipziger Str. 44, 39120 Magdeburg, Germany

[6]UCL Institute of Neurology, University College of London, Queen Square, London WC1N 3BG, UK

[7]Lead Contact

*Correspondence: j.wlodarczyk@nencki.gov.pl (J.W.), ponimaskin.evgeni@mh-hannover.de (E.P.)

http://dx.doi.org/10.1016/j.celrep.2017.05.023

SUMMARY

Rewiring of synaptic circuitry pertinent to memory formation has been associated with morphological changes in dendritic spines and with extracellular matrix (ECM) remodeling. Here, we mechanistically link these processes by uncovering a signaling pathway involving the serotonin 5-HT7 receptor (5-HT7R), matrix metalloproteinase 9 (MMP-9), the hyaluronan receptor CD44, and the small GTPase Cdc42. We highlight a physical interaction between 5-HT7R and CD44 (identified as an MMP-9 substrate in neurons) and find that 5-HT7R stimulation increases local MMP-9 activity, triggering dendritic spine remodeling, synaptic pruning, and impairment of long-term potentiation (LTP). The underlying molecular machinery involves 5-HT7R-mediated activation of MMP-9, which leads to CD44 cleavage followed by Cdc42 activation. One important physiological consequence of this interaction includes an increase in neuronal outgrowth and elongation of dendritic spines, which might have a positive effect on complex neuronal processes (e.g., reversal learning and neuronal regeneration).

INTRODUCTION

Dendritic spines that host excitatory synaptic contacts can undergo morphological changes in response to stimuli that trigger long-term alterations in transmission efficacy. This structural remodeling leads to neural network rewiring on a larger scale, which is a commonly perceived substrate of learning and memory formation and, in some cases of pathological changes, in the brain (Sala and Segal, 2014). This process is regulated by signaling pathways that engage the neurotransmitter serotonin (5-hydroxytryptamine [5-HT]) and the extracellular matrix (ECM) (Udo et al., 2005; Dityatev et al., 2010). However, the mechanism underlying the molecular interactions between the ECM and serotonin-mediated signaling in neurons in situ has remained unknown.

The serotonin receptor subtype 5-HT7 has recently been reported to play a significant role in pathological forms of synaptic plasticity, such as those associated with anxiety and depression (Hedlund, 2009; Matthys et al., 2011). At the molecular level, 5-HT7 receptors (5-HT7Rs) prompt the formation of cyclic AMP (cAMP) by activating adenylyl cyclase via the stimulatory $G\alpha_s$ protein (Norum et al., 2003). 5-HT7R-mediated activation of the heteromeric $G\alpha_{12}$ protein results in selective activation of small guanosine triphosphatases (GTPases) of the Rho family, which, in turn, triggers pronounced changes in cellular morphology, including synaptogenesis (Kvachnina et al., 2005; Kobe et al., 2012).

Among numerous ECM components and modifiers that play a part in long-term memory and synaptic plasticity, matrix metalloproteinase 9 (MMP-9) has recently emerged as a key molecule (Huntley, 2012). MMP-9 may contribute to dynamic remodeling of the ECM via cleaving ECM components, such as laminin and aggrecan, and cell adhesion molecules (Dityatev et al., 2010; Ethell and Ethell, 2007). At the same time, MMP-9 signaling has been shown to contribute to the formation and maintenance of dendritic spines (Wang et al., 2008; Michaluk et al., 2011; Szepesi et al., 2013, 2014) and, possibly, dendritic protrusions associated with neuropsychiatric disorders (for a review, see Stawarski et al., 2014a). Notably, elevated levels of MMP-9 were found in the blood of patients with clinical depression (Rybakowski et al., 2013).

Notwithstanding its apparent significance, the causal link between MMP-9 activity and structural plasticity has remained

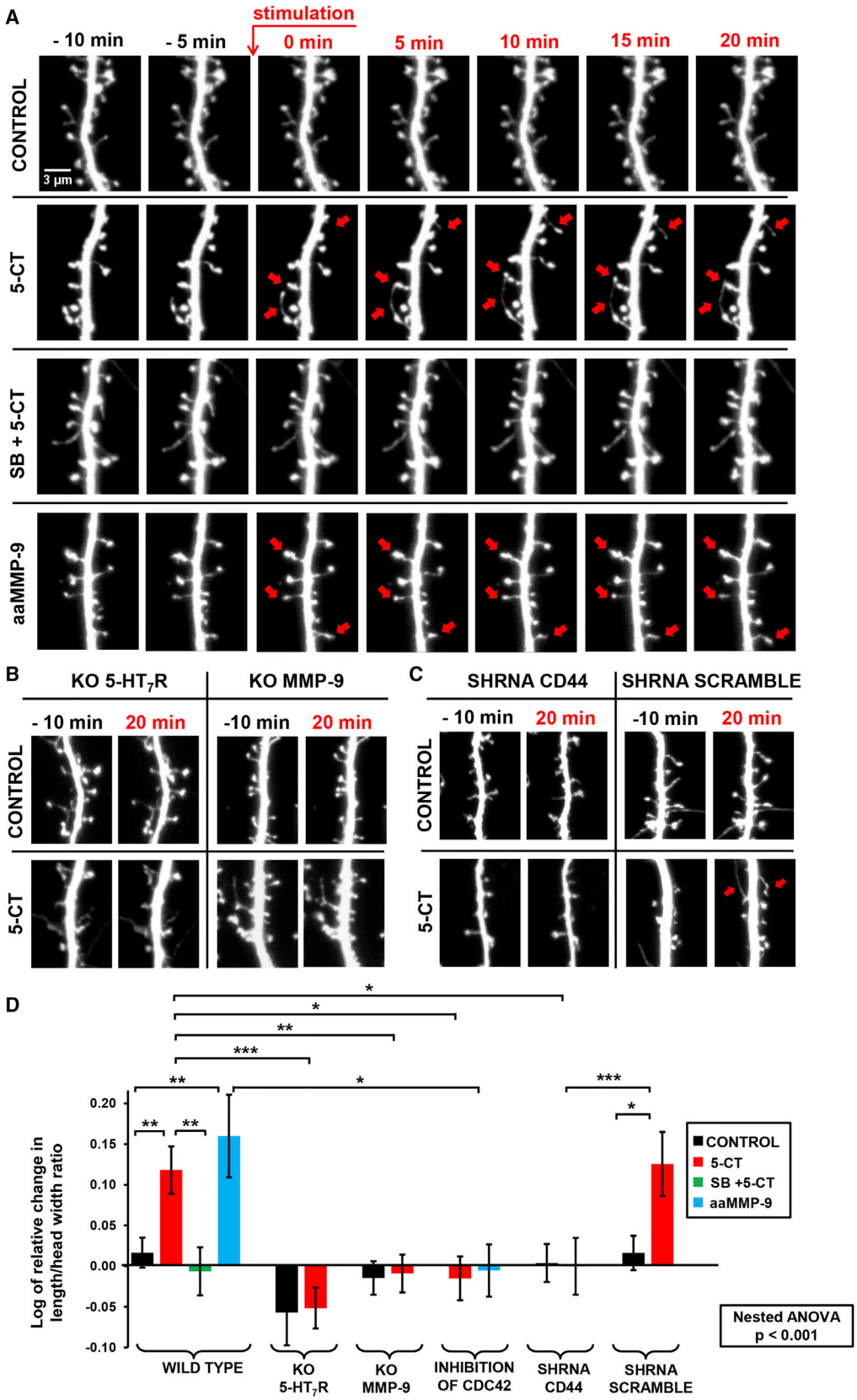

(legend on next page)

poorly understood. Several cell adhesion proteins have been proposed as the substrates of MMP-9 in neurons (Michaluk et al., 2007; Bajor et al., 2012), but their roles in the structural plasticity of dendritic spines are yet to be ascertained. Here we identify the transmembrane protein CD44, which connects the neuronal cytoskeleton to the ECM, as a previously unknown neuronal MMP-9 substrate. CD44 is a major receptor for hyaluronan, which is the main component of the neural ECM influencing both structural and functional aspects of neuronal plasticity (Kochlamazashvili et al., 2010). The extracellular N-terminal CD44 domain is responsible for binding hyaluronic acid, osteopontin, collagen, laminin, and fibronectin (Carter and Wayner, 1988; Weber et al., 1996). The C-terminal cytoplasmic region interacts with different cytoskeleton-associated proteins, such as ankyrin (Kalomiris and Bourguignon, 1988) and ezrin/radixin/moesin (ERM) proteins (Duterme et al., 2009). CD44-mediated signaling also modulates the activity of small Rho GTPases (Bourguignon et al., 2005). In neurons, GTPases of the Rho family play a pivotal role in spino- and synaptogenesis (Jontes and Smith, 2000). One omnipresent member of the Rho GTPase family acting as a positive regulator of filopodium formation, neurite outgrowth, and growth cone protrusion is Cdc42 (Brown et al., 2000). Cdc42 has also emerged as an important modulator of structural plastic changes in dendrites and dendritic spines (Newey et al., 2005).

In the present study, we establish a causal link between 5-HT7R-mediated signaling and extracellular cleavage of CD44 by MMP-9, which, in turn, engages Cdc42 to regulate synaptogenesis, LTP, and the structural plasticity of dendritic spines.

RESULTS

5-HT7R Stimulation Triggers Dendritic Spine Morphogenesis, which Requires MMP-9 Activity and Depends on Cdc42

To test whether and how 5-HT7R activation engages MMP-9-dependent dendritic spine morphogenesis, we monitored spine morphology using the length over head width ratio as a scale-free parameter in real time in dissociated hippocampal cultures expressing red fluorescent protein (RFP). The 5-HT7R agonist 5-carboxamidotryptamine (5-CT) (10 μM, 20 min) triggered a prominent elongation of dendritic spines shortly after stimulation (Figure 1A; see Figure 1D for a statistical summary), consistent with previous observations (Kvachnina et al., 2005). These changes were receptor-specific because they were blocked by the high-affinity 5-HT7R antagonist SB 269970 (Figures 1A and 1D). Similar spine elongation was observed after application of auto-activating MMP-9 (aaMMP-9, 400 ng/ml, 20 min) (Figures 1A and 1D). In contrast, no spine elongation was detected in cultures prepared from MMP-9 knockout (KO) (Ducharme et al., 2000) and 5-HT7R KO (Hedlund et al., 2003) mice (Figures 1B and 1D), confirming specific involvement of 5-HT7R/MMP-9 signaling in dendritic spine changes. Noteworthy is that the increase in the spine length obtained after application of aaMMP-9 or upon 5-HT7R stimulation was accompanied by decreased spine head width (Figure S1B).

We have previously suggested, based on sample comparison data, that the small GTPase Cdc42 is a downstream effector of 5-HT7R signaling involved in neurite outgrowth (Kvachnina et al., 2005). Strikingly, pretreatment of neurons with the specific Cdc42 inhibitor ZCL278 (Friesland et al., 2013) completely prevented dendritic spine elongation in response to either 5-HT7R stimulation or aaMMP-9 treatment (Figures S1A and 1D). Because MMP-9 is a known ECM modifier (Dityatev et al., 2010; Huntley, 2012; Ethell and Ethell, 2007), we asked whether the ECM can also be involved. For that, we focused on CD44, the receptor for a major ECM component, hyaluronan, connecting the ECM with the intracellular signaling pathway involved in activation of the small Rho GTPases. Silencing of neuronal CD44 expression via specific short hairpin RNAs (shRNAs) (Skupien et al., 2014) abrogated the 5-HT7R stimulation-induced elongation of dendritic spines, whereas neurons transfected with a plasmid encoding a scrambled shRNA displayed elongation similar to that in non-transfected neurons (Figures 1C and 1D).

We next sought to test whether 5-HT7R activation induced morphological alterations in organized brain tissue and whether dendritic spines undergoing such changes, if any, indeed represent functional synapses. We therefore turned to the preparation of organotypic hippocampal slices and held imaged pyramidal cells in whole-cell mode to probe their individual dendritic spines

Figure 1. Changes in Spine Shape after 5-HT7R Stimulation Depend on MMP-9, CD44, and Cdc42

(A) RFP-transfected hippocampal WT neurons captured during live imaging under control conditions and after treatment with 5-CT, SB 269970 (SB) + 5-CT, and aaMMP-9. The arrows indicate the locations of spines that underwent structural plasticity.

(B) Hippocampal neurons from 5-HT7R KO mice and MMP-9 KO mice stimulated with 5-CT.

(C) Hippocampal neurons co-transfected with shRNA against CD44 or scramble shRNA and stimulated with 5-CT.

(D) Quantification of changes in the length/head width ratio of dendritic spines 20 min after stimulation with 5-CT or aaMMP-9. 5-CT application (0.12 ± 0.03, $n_{cells/spines}$ = 25/560) increases the ratio compared with control neurons (0.02 ± 0.02, $n_{cells/spines}$ = 19/392). Treatment with SB269970 abolished these changes (−0.01 ± 0.03, $n_{cells/spines}$ = 16/326). Treatment with aaMMP-9 caused spine elongation (0.16 ± 0.05, $n_{cells/spines}$ = 15/408). Incubation of 5-HT7R KO neurons or MMP-9 KO neurons with 5-CT did not influence spine morphology (5-HT7R KO + 5-CT, −0.05 ± 0.03, $n_{cells/spines}$ = 26/447; 5-HT7R KO control, −0.06 ± 0.04, $n_{cells/spines}$ = 19/468; MMP-9 KO + 5-CT, −0.01 ± 0.02, $n_{cells/spines}$ = 12/429; MMP-9 KO control, −0.02 ± 0.02, $n_{cells/spines}$ = 15/631). Pretreatment of the neurons with Cdc42 inhibitor prevented the 5-CT changes and aaMMP-9 mediated changes, respectively (−0.02 ± 0.03, $n_{cells/spines}$ = 9/361 and −0.01 ± 0.03, $n_{cells/spines}$ = 8/404). 5-HT7R stimulation in neurons transfected with CD44 shRNA did not influence spine shape (0.00 ± 0.03, $n_{cells/spines}$ = 17/490) compared with control neurons (0.0 ± 0.02, $n_{cells/spines}$ = 11/391). Spine elongation after 5-CT treatment in neurons transfected with scramble shRNA was similar to non-transfected neurons (0.12 ± 0.04, $n_{cells/spines}$ = 13/417). A significantly higher length/head width ratio was observed in neurons transfected with scramble shRNA and treated with 5-CT compared with non-stimulated cells (0.02 ± 0.02, $n_{cells/spines}$ = 10/402). The quantification of spines was done using a cell as the statistical unit. The data are expressed as mean ± SEM (*p < 0.05, **p < 0.01, ***p < 0.001.).

See also Figure S1.

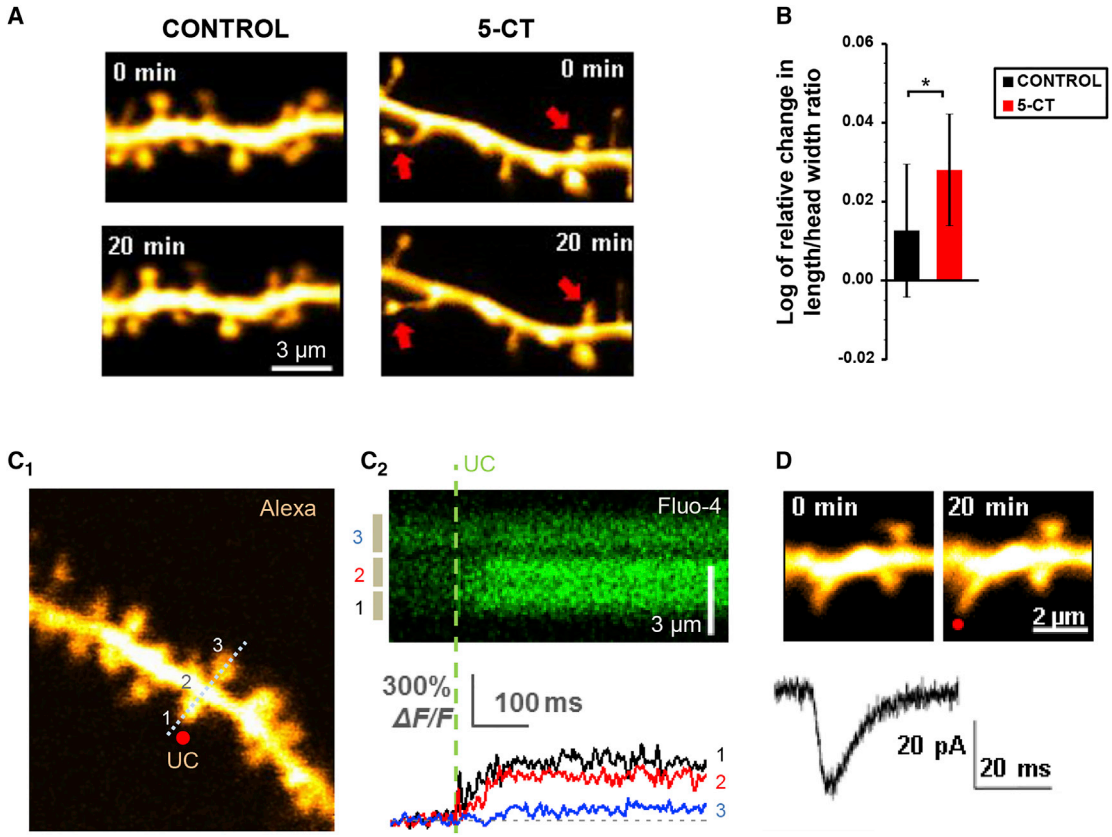

Figure 2. Probing Synaptic Function and 5-CT Effects at Dendritic Spines in Organotypic Hippocampal Slices

(A) Monitoring of dendritic spine morphology in control conditions and after 5-CT application as indicated. Red arrows, examples of spines with altered morphology after 20 min in 5-CT.

(B) Changes in spine shape over 20 min under control conditions and after 5-CT application as indicated. Columns ± error bars, mean ± SEM; *$p < 0.03$.

(C) Two-photon spot uncaging of glutamate triggers postsynaptic Ca^{2+} entry at an immediately adjacent dendritic spine.

(C1) Dendritic fragment of interest (example, Alexa channel) with uncaging (UC) spot, line scan positioning (dotted line), and three regions of interests (1, 2, and 3—immediate spine, dendritic stem, and neighboring spine, respectively) as indicated.

(C2) Postsynaptic Ca^{2+} transients (top, line scan; bottom, traces; as indicated) triggered by glutamate UC (onset shown by the dotted line) originate in the immediately adjacent spine (1) followed by rises in neighboring dendritic compartments (2 and 3) as indicated.

(D) Probing postsynaptic glutamatergic responses in dendritic spines that undergo 5-CT-induced morphological changes (example). Top: dendritic fragment with the spine of interest before and 20 min after 5-CT application as indicated (example, Alexa channel). Red dot, position of spot uncaging. Bottom: an electrical response in the postsynaptic spine to glutamate spot uncaging (voltage-clamp at −70 mV).

with two-photon spot uncaging of extracellular glutamate. First we confirmed that, with these experimental settings, 5-CT induced a significant increase in the spine elongation factor (Figures 2A and 2B), which was fully consistent with that in the experiments in dissociated cultures (Figure 1). The average quantitative effect was somewhat smaller (albeit statistically significant) than that in cultured cells, most likely because of the whole-cell pipette dialysis, which could potentially dilute cellular metabolites involved in the morphogenesis. Reassuringly, 2.9% of analyzed spines increased their elongation factor by more than 3-fold after 5-CT treatment, whereas, in control experiments, this fraction (because of baseline shape fluctuations) was only 0.8%.

Second, we used postsynaptic Ca^{2+} imaging to confirm that our uncaging protocol triggers Ca^{2+} responses in individual dendritic spine heads rather than in dendrites in bulk (Figure 2C). In these tests, the evoked Ca^{2+} signal onset in the spine head was in advance of that in the dendrite, thus indicating the spine head origin of the Ca^{2+} entry, as shown by us earlier in experiments involving optical quantal analysis (Boddum et al., 2016). Finally, we found that, in all tested spines that underwent visible 5-CT-induced changes, glutamate uncaging evoked a robust postsynaptic electrical response (Figure 2D) entirely consistent with the endogenously evoked excitatory postsynaptic currents (EPSCs) documented routinely in similar settings (Rusakov and Fine, 2003).

These experiments suggest that 5-HT7R, MMP-9, CD44, and Cdc42 represent components of a molecular cascade required for the triggering of morphological changes in dendritic spines and that, in all likelihood, these modified spines represent functional synapses. Therefore, we next focused on the underlying molecular machinery.

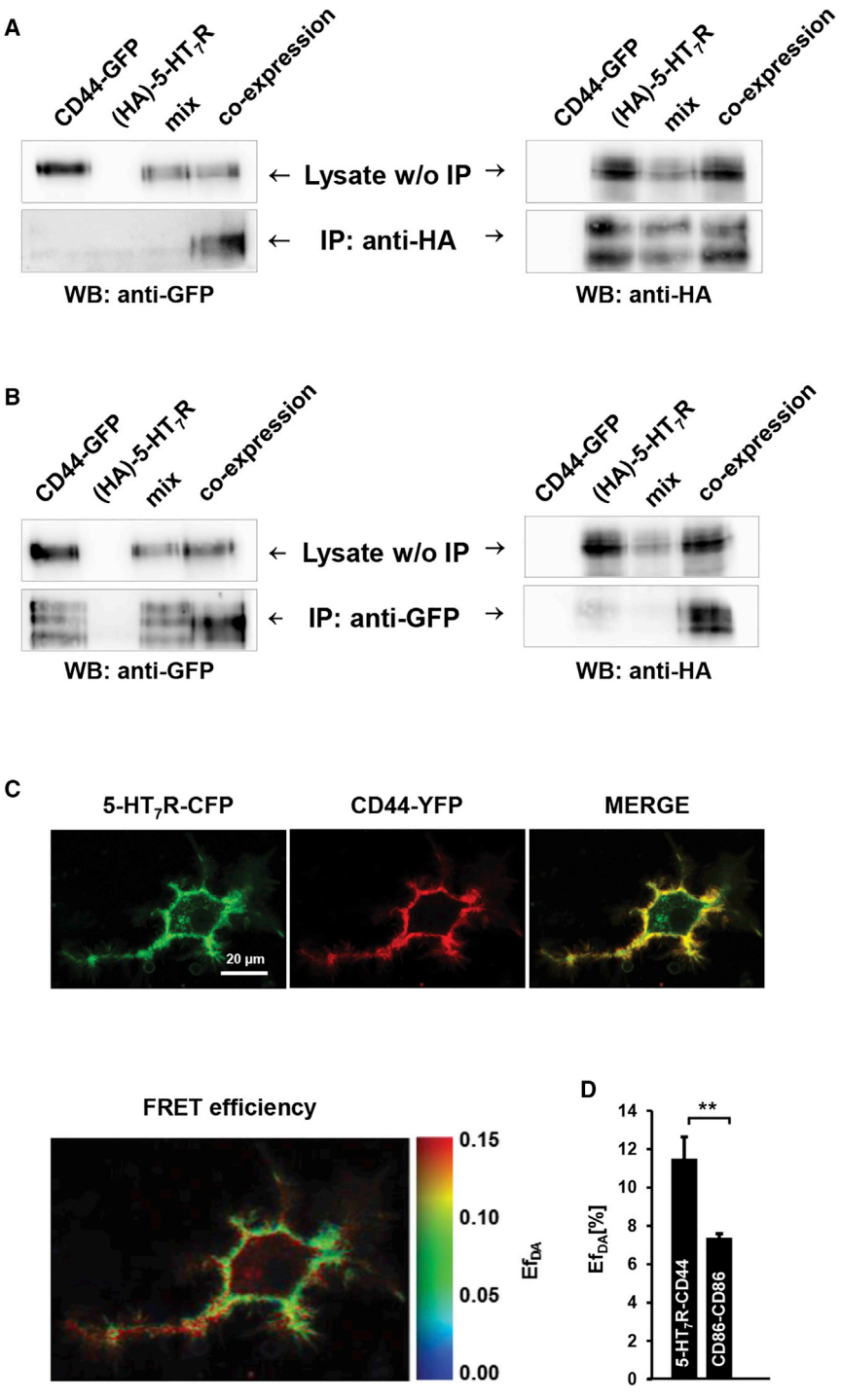

Figure 3. Interaction between 5-HT7R and CD44 in Neuroblastoma N1E-115 Cells

(A and B) CoIP of recombinant HA-tagged 5-HT7Rs (HA-5-HT7R) and CD44-GFP in N1E cells. A mixture of cells that expressed each individual protein (mix) or cells that co-expressed both proteins (co-expression) were subjected to immunoprecipitation (IP) with anti-HA (A) or anti-GFP (B) antibody, followed by western blot (WB) analysis with anti-GFP (left) and anti-HA (right) antibodies. Top: the expression of proteins before IP (Lysate w/o IP). Bottom: the expression of proteins after IP. The results are representative of at least four independent experiments.

(C) Specific interaction between 5-HT7R tagged with CFP (5-HT7R-CFP) and CD44-YFP. Cells that co-expressed 5-HT7R-CFP and CD44-YFP were analyzed using the lux-FRET method after confocal microscopy. Top: distribution of 5-HT7R-CFP (donor), CD44-YFP (acceptor), and merged images calculated by linear unmixing of the fluorescence emission spectra. Bottom: the apparent FRET efficiency (Ef_{DA}). A representative cell is shown. See also Figures S2 and S3.

(D) Quantification of FRET efficiencies (Ef_{DA}) between 5-HT7R-CFP and CD44-YFP (Ef_{DA} = 11.51% ± 1.12%, n_{Cell} = 7) as well as CD86-CFP and CD86-YFP (Ef_{DA} = 7.37% ± 0.22%, p = 0.0029, n_{Cell} = 7). Data represent mean ± SEM (n = 7, **p < 0.05, Student's t test).

cells co-expressing hemagglutinin (HA)-tagged 5-HT7Rs (HA-5-HT7Rs) and GFP-tagged CD44 (CD44-GFP), CD44 interacted with HA-5-HT7R (Figures 3A and 3B). The specificity of coIP was confirmed by analysis in cells expressing either HA-5-HT7Rs only, CD44-GFP only, or a mixture of these cells performed before lysis (Figures 3A and 3B).

CoIP requires solubilization and concentration of the membrane proteins, which can result in artificial aggregation of receptors (Harrison and van der Graaf, 2006). To overcome this limitation and to analyze the oligomerization behavior of 5-HT7Rs and CD44 in living cells, we applied a fluorescence resonance energy transfer (FRET)-based approach. FRET efficiencies between CFP-labeled 5-HT7Rs (5-HT7R-CFP, donor) and yellow fluorescent protein (YFP)-labeled CD44 (CD44-YFP, acceptor) were measured in living N1E-115 using the linear unmixing (lux)-FRET method; this approach is capable of detecting the physical proximity of individual molecules on the nanoscale (Wlodarczyk et al., 2008). These experiments revealed that 5-HT7R-CFP and CD44-YFP were co-localized at the plasma membrane (Figure 3C). The donor molar fraction x_D, which indicates the ratio between donor and acceptor molecules, was in the range of 0.5, demonstrating

Recombinant 5-HT7Rs and CD44 Interact on the Nanoscale

Both 5-HT7R and CD44 are integral membrane proteins residing at the plasma membrane. Therefore, we first investigated whether the signaling described above involves direct interactions between 5-HT7Rs and CD44. In co-immunoprecipitation (coIP) experiments performed in neuroblastoma N1E-115

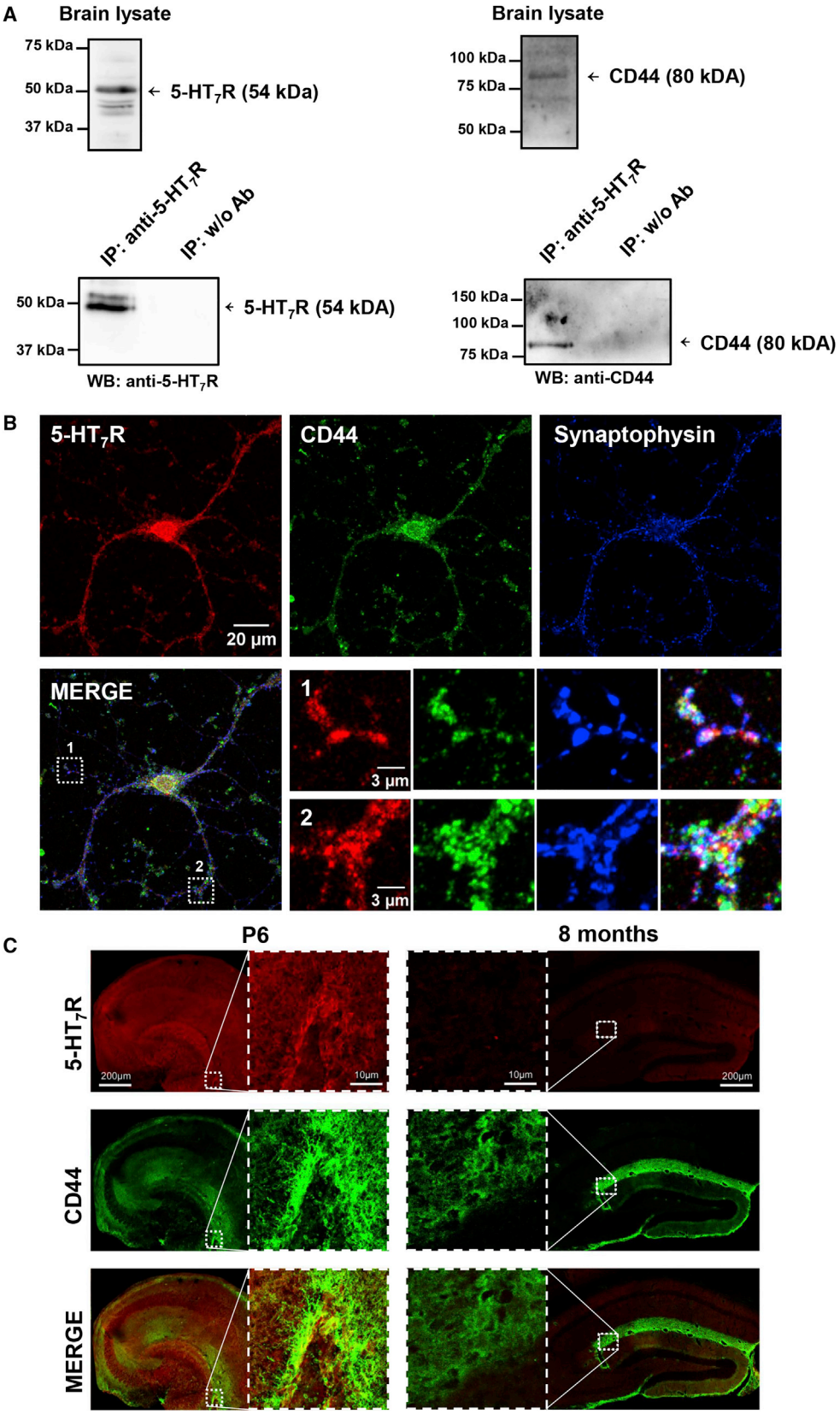

(legend on next page)

that both proteins were expressed at similar concentrations (Figure S2). The lux-FRET analysis revealed high apparent FRET efficiency, Ef_{DA} (Ef_{DA} = 11.51% ± 1.12%), for 5-HT7R-CFP and CD44-YFP. In contrast, cells expressing both CD86-CFP and CD86-YFP, which have been considered monomeric (Dorsch et al., 2009), showed much lower Ef_{DA} values (Figure 3D). Moreover, the Ef_{DA} values of CD86 showed a linear dependence on the relative expression level (Figure S3A), pointing to a random rather than a specific occurrence of a close molecular neighborhood, most likely because of the high protein concentration at the plasma membrane. An additional FRET analysis for 5-HT7R-CFP and CD44-YFP performed at a fixed donor/acceptor ratio showed no correlation with the expression level (Figure S3A). In other words, the FRET efficiencies were independent of donor/acceptor concentrations, thus confirming a specific, as opposed to random, interaction between the two proteins (James et al., 2006).

These combined data demonstrate an interaction between 5-HT7Rs and CD44 in the nanodomain on the scale of minutes. Intriguingly, this interaction occurs independently of the 5-HT7R activation/inactivation because neither agonist nor antagonist alter the Ef_{DA} value (Figure S3B).

Endogenous 5-HT7Rs and CD44 Form a Protein Complex in the Mouse Brain

We next asked whether the endogenous 5-HT7Rs and CD44 interact to form a protein complex. Because the expression of 5-HT7Rs peaks during early postnatal stages (Kobe et al., 2012), we analyzed whole-brain lysates prepared from wild-type (WT) and 5-HT7R-deficient mice at post-natal day 6 (P6) by coIP. These experiments demonstrated a direct interaction of endogenous CD44 and the 5-HT7R (Figure 4A; Figure S4A). A possibility for interaction of CD44 and 5-HT7R at the cellular level was verified by immunofluorescence analysis performed in cultures of dissociated hippocampal neurons using antibodies against the 5-HT7R, CD44, and synaptophysin, which was used as a presynaptic marker (Kobe et al., 2012). The 5-HT7R was co-localized with CD44 at synapses (Figure 4B). The specificity of the anti-5-HT7R antibody was verified using neurons transfected with the shRNA against 5-HT7R (Figure S4B).

To verify co-localization of endogenous 5-HT7Rs and CD44 during development in situ, immunohistochemistry was performed in hippocampal slices prepared from 6-day-old and 8-month-old mice. 5-HT7Rs and CD44 were highly co-localized in the CA1, CA2, and CA3 regions and the dentate gyrus of the hippocampus in P6 mice (Figure 4C). Consistent with our previous observations (Kobe et al., 2012), the expression of the 5-HT7R was drastically downregulated in the hippocampus in 8-month-old mice (Figure 4C), whereas changes in CD44 expression were less prominent.

Stimulation of 5-HT7Rs Leads to MMP-9 Activation

To test whether 5-HT7R stimulation activates MMP-9, we used three different approaches: visualization of gelatinase (MMP-9 and MMP-2) activity at the single-spine level in living cells, analysis of total MMP-9 activity via gel zymography, and ratiometric measurements using a FRET-based MMP-9 activity biosensor.

In the first approach, hippocampal neurons visualized by RFP expression were pre-incubated with the fluorogenic substrate dye-quenched (DQ)-gelatin. Upon 5-CT application, we observed significantly enhanced gelatinase activity in dendrites of WT neurons, particularly at the newly elongated dendritic spines (Figure 5A, white arrows). In contrast, in cells that were either pretreated with the highly selective 5-HT7R antagonist SB 269970 (10 min) or isolated from 5-HT7R KO mice or MMP-9 KO mice, 5-CT treatment had no effect on gelatinase activity (Figures 5A and 5B).

In the second approach, total MMP-9 activity was evaluated using gel zymography (Vandooren et al., 2013). We found that 5-CT application significantly increased MMP-9 activity 20 min post-stimulus compared with the control samples, whereas constitutive receptor activity (which was verified by treatment with the receptor antagonist SB 269970) was not involved in MMP-9 activation (Figures 5C and 5D). Again, pretreatment with the 5-HT7R antagonist SB 269970 or using cells from 5-HT7R KO mice completely abolished the effect of 5-CT and dropped MMP9 activity to the levels seen in control experiments (Figures 5C and 5D; Figure S5).

To evaluate the 5-HT7R-mediated activation of MMP-9 in real time, live-cell imaging was performed in hippocampal neurons transfected with the FRET-based MMP-9 activity biosensor (Stawarski et al., 2014b). In this construct, MMP-9 activation can be monitored by observing a decrease of the Venus/mTFP1 fluorescence intensity ratio mediated by MMP-9 sensor cleavage (Figure S6A). To verify the sensor's responsiveness, WT neurons were treated with aaMMP-9, resulting in cleavage of the biosensor (Figure 5E) and a significant reduction in the Venus/mTFP1 fluorescence intensity ratio relative to control cells (Figures 5F and 5G). 5-CT treatment of sensor-expressing WT neurons also resulted in a significant decrease in the Venus/mTFP1 fluorescence intensity ratio (Figures 5E–5G). In contrast, pre-incubation of 5-HT7Rs with SB 269970 abolished the effect of 5-CT on biosensor cleavage (Figure 5E–5G), indicating the importance of 5-HT7R for activation of endogenous MMP-9.

Figure 4. Interaction between Endogenous 5-HT7R and CD44 in the Brain

(A) CoIP between 5-HT7R and CD44 in brain lysates. Whole-brain homogenates were prepared from P6 mice and subjected to IP with anti-5-HT7R antibody or without antibody (w/o Ab), followed by WB analysis with anti-5-HT7R and anti-CD44 antibodies. Top: the expression of proteins before IP. Bottom: the expression of proteins after IP. Results are representative of at least four independent experiments. For control of the specificity of anti-5-HT7R antibody, see Figure S4A.

(B) Co-localization of 5-HT7R, synaptophysin, and CD44 in primary hippocampal neurons. Neurons were fixed on day in vitro 12 (DIV12), incubated with specific antibodies, and analyzed for expression of 5-HT7R, CD44, and the synaptic marker synaptophysin using confocal microscopy. Top: the expression of 5-HT7R (red), CD44 (green), and synaptophysin (blue) of a representative neuron. Bottom: merged image and a magnified view of two representative dendrites. See also Figure S4B.

(C) Co-localization of 5-HT7R and CD44 in hippocampal slices. Brain slices from 6-day-old and 8-month-old mice were subjected to immunohistochemistry for the detection of 5-HT7R (red) and CD44 (green), followed by confocal microscopy.

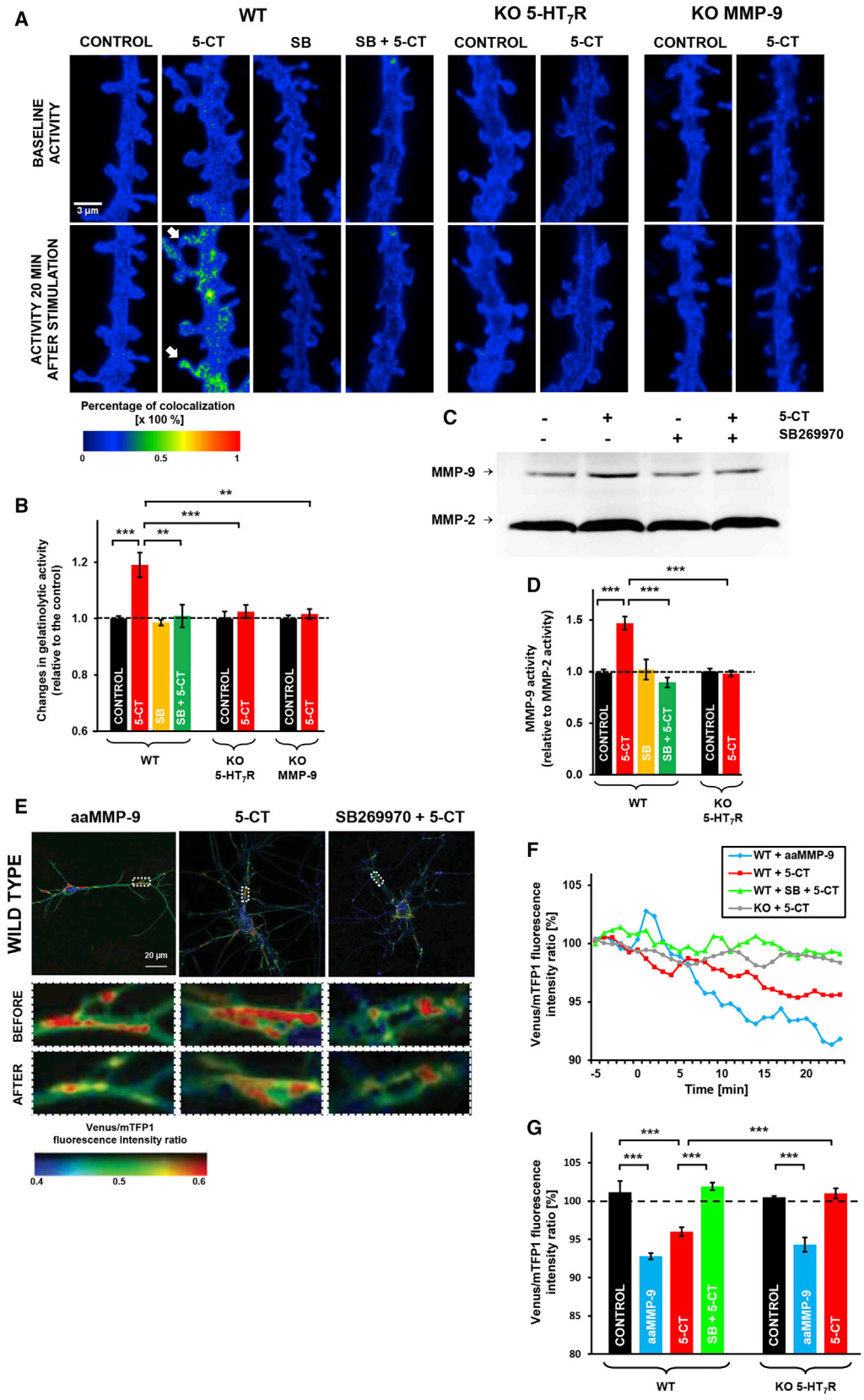

(legend on next page)

This was further confirmed by the observation that no cleavage of the MMP-9 activity biosensor was found upon 5-CT application in neurons isolated from 5-HT7R KO mice (Figures 5F and 5G; Figure S6B). To determine whether the MMP-9 biosensor can still be cleaved in 5-HT7R KO neurons, these cells were treated with aaMMP-9, resulting in a significant decrease in the Venus/mTFP1 fluorescence intensity ratio (Figures 5F and 5G).

MMP-9 Cleaves the Extracellular Domain of CD44

It has been shown that CD44 can be proteolytically cleaved at the ectodomain through membrane-anchored metalloproteases and that CD44 cleavage plays a critical role in the regulation of cellular morphology (Okamoto et al., 1999). Having demonstrated that 5-HT7R stimulation leads to MMP-9 activation, we asked whether CD44 is a cleavage substrate of MMP-9. For that, homogenates were prepared from hippocampal tissue from P6 mice and incubated with recombinant aaMMP-9 (400 ng/mL). Western blot analysis revealed an increase in both the 40- and 55-kDa cleavage products of CD44, identified with an antibody directed against the extracellular domain of CD44, and a 25-kDa protein band that was recognized by an antibody against the intracellular domain (Figure S7A). These data suggest that CD44 might be a substrate for MMP-9 in the brain. As a positive control for MMP-9 activity, we used β-dystroglycan, a well-established MMP-9 substrate (Figure S7A; Michaluk et al., 2007). To investigate the MMP-9-mediated proteolytic cleavage of CD44 in molecular detail, hippocampal neurons were transfected with the CD44 shedding reporter, which enables the visualization of CD44 cleavage in living cells (Marrero-Diaz et al., 2009). In this construct, CD44 is fused to mOrange at the N terminus and GFP at the C terminus. After cleavage of the extracellular domain of CD44, mOrange is released, resulting in a decrease in the mOrange/GFP fluorescence intensity ratio (Figure S7B). After 20-min aaMMP-9 treatment of WT neurons expressing the CD44 shedding reporter, we observed a significant decrease in the mOrange/GFP fluorescence intensity ratio compared with controls (Figures S7C and S7D). Treatment with an inactive mutant of MMP-9 (iaMMP-9) did not induce any changes in the mOrange/GFP ratio (Figures S7C and S7D). These combined data suggest that MMP-9 can proteolytically cleave CD44 at its extracellular domain.

Stimulation of 5-HT7Rs Leads to MMP-9-Mediated CD44 Cleavage

To understand whether 5-HT7R activation leads to CD44 cleavage and whether this process occurs in an MMP-9-dependent manner, we performed time-lapse analysis of the cleavage of the CD44 shedding reporter in WT neurons and neurons isolated from 5-HT7R KO and MMP-9 KO mice. Application of 5-CT resulted in profound cleavage of the CD44 shedding reporter, as assessed by a decreased mOrange/GFP fluorescence intensity ratio (Figure 6A), an effect similar to that obtained after aaMMP-9 application (Figures S7C and S7D). Importantly, pretreatment with either the 5-HT7R antagonist SB 269970 (10 min) or the specific inhibitor of MMP-9 enzymatic activity inhibitor I (30 min) reduced the cleavage of CD44 to the baseline level (Figures 6A and 6B). Noteworthy is that 5-CT treatment of neurons isolated from either 5-HT7R KO or MMP-9 KO mice had no effect on CD44 cleavage (Figure 6). At the same time, cleavage of CD44 was still observed in both KO 5-HT7R neurons and KO MMP-9 neurons upon aaMPP-9 application (Figure 6A), thus ruling out concomitant effects pertinent to the knockout models. In summary, these results strongly indicate that stimulation of the 5-HT7R leads to CD44 cleavage in neurons in an MMP-9-dependent manner.

The 5-HT7R/MMP-9/CD44 Signaling Cascade Contributes to the Expression of LTP

Our previous study revealed an impairment of CA1 LTP after activation of the 5-HT7R by 5-CT in organotypic hippocampal cultures (Kobe et al., 2012). Here we found a similar effect at CA3-CA1 synapses in acute hippocampal slices (Figure 7A) and sought to investigate the roles of MMP-9 (extracellular part) and Cdc42 (intracellular part) in the underlying mechanisms.

Figure 5. Stimulation of 5-HT7Rs Increases the Activity of MMP-9 on Elongating Dendritic Spines

(A) Time-lapse images of dendrites before and 20 min after 5-CT treatment. The co-localization map shows an increase in gelatinase activity at elongating dendritic spines 20 min after 5-CT treatment in WT neurons (white arrows). The color-coded bar indicates the percentage of co-localization.

(B) Quantification of gelatinase activity on dendritic spines. Intensities are presented relative to controls. 5-CT treatment (1.19 ± 0.04, $p < 0.001$, $n_{cell} = 24$) results in a significant increase in gelatinase activity, whereas SB269970 (0.99 ± 0.01, $n_{cell} = 18$) and SB269970 + 5-CT treatment (1.01 ± 0.04, $n_{cell} = 21$) did not change gelatinase activity. 5-CT stimulation of neurons from 5-HT7R KO mice and MMP-9 KO mice did not induce changes in gelatinase activity (5-HT7 KO, 1.03 ± 0.02, $p = 0.8$, $n_{cell} = 24$; MMP-9 KO, 1.02 ± 0.02, $p = 0.4$, $n_{cell} = 18$; $^{**}p < 0.01$, $^{***}p < 0.001$).

(C) Gelatinase activity of hippocampal neurons exposed to 5-CT for 20 min. A representative gel zymogram is shown (see also Figure S5).

(D) Quantification of the MMP-9/MMP-2 activity ratio in the zymogram shown in (C) after 5-CT treatment revealed a significant increase (1.47 ± 0.06, $p < 0.0001$, $n = 16$). The MMP-9/MMP-2 ratio did not change in cells treated with SB 269970 (1.02 ± 0.10, $n = 5$) or treated with SB 269970 + 5-CT (0.89 ± 0.05, $n = 13$) as well as in neurons isolated from KO 5-HT7R mice upon 5-CT stimulation. All data are expressed as mean ± SEM. $^{***}p < 0.001$.

(E) Live-cell imaging of FRET-based MMP-9 activity biosensor (see also Figure S6A) after treatment with aaMMP-9, 5-CT, or 5-CT + SB 269970 for 20 min. A representative image for each condition shows the mean Venus/mTFP1 fluorescence intensity ratio before treatment. The magnified view of the region of interest is shown as the mean intensity ratio before and after treatment (see also Figure S6B).

(F) The representative time courses of the normalized Venus/mTFP1 fluorescence intensity ratio are depicted for the indicated regions of interest. The time point of treatment is indicated by the arrow.

(G) Quantification of normalized fluorescence intensity ratios of WT and 5-HT7R KO neurons after the indicated treatments. Treatment of WT neurons with aaMMP-9 results in significant reduction in the Venus/mTFP1 fluorescence intensity ratio to 92.8% ± 0.41% ($p < 0.001$) relative to control cells (101.2% ± 1.45%). 5-CT treatment of WT neurons significantly decreases the Venus/mTFP1 fluorescence intensity ratio to 96.0% ± 0.58% ($p < 0.001$), and pretreatment with SB 269970 abolished this effect (101.9% ± 0.49%). No changes in Venus/mTFP1 fluorescence intensity ratio were found upon 5-CT application in 5-HT7R KO neurons (101.0% ± 0.67% for 5-CT treatment versus 100.5% ± 0.16% for control), whereas treatment with aaMMP-9 results in a significant decrease in the Venus/mTFP1 ratio to 94.3% ± 0.93% ($p < 0.001$). The data are expressed as the mean ± SEM of different cells ($n \geq 3$, $^{***}p < 0.001$, ANOVA).

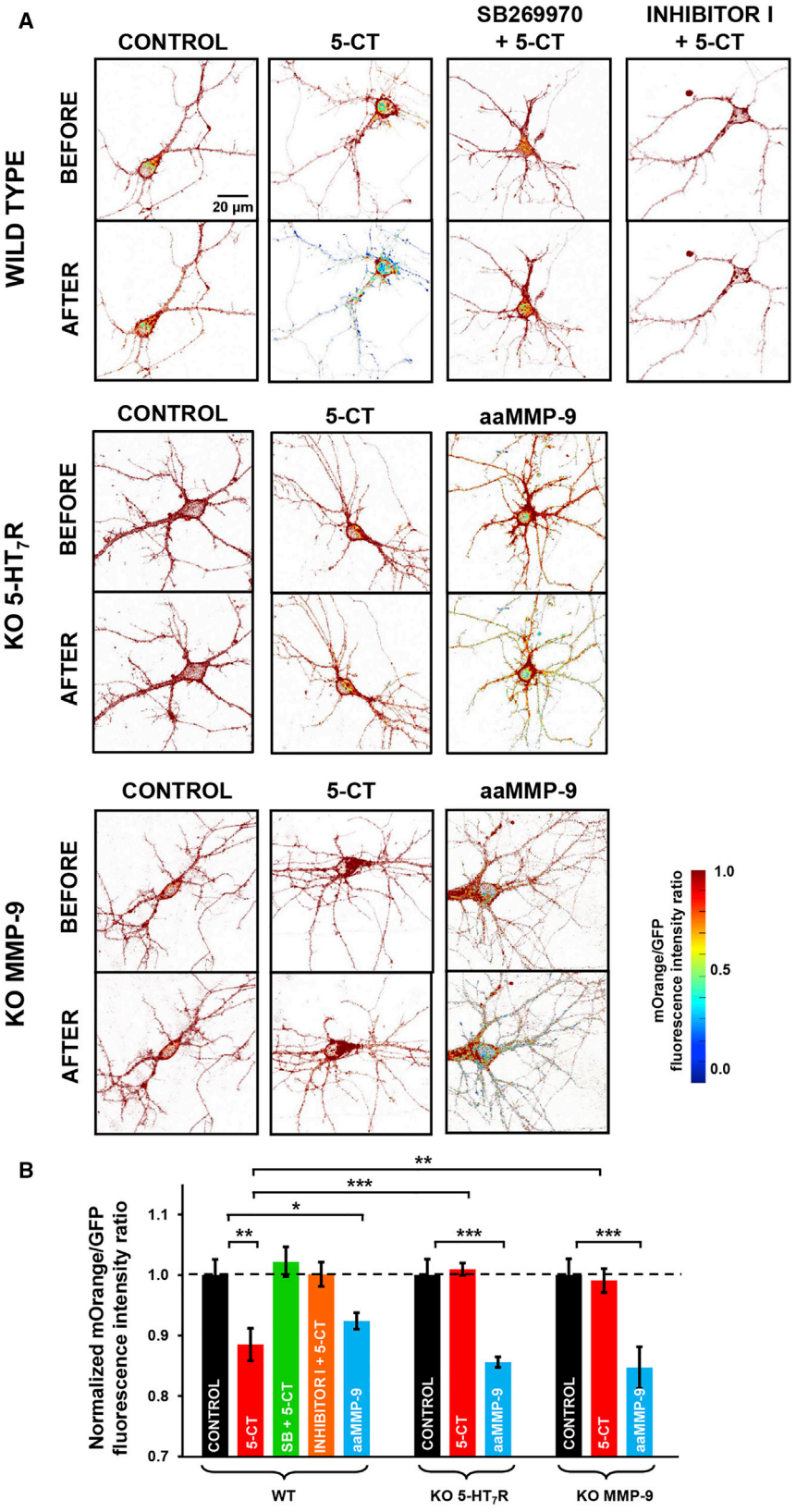

Figure 6. 5-HT7R Stimulation Leads to MMP-9-Dependent Cleavage of CD44

(A) Representative images of living neurons expressing the CD44 shedding reporter are shown as the mOrange/GFP fluorescence intensity ratio. 5-CT treatment results in a decrease in the mOrange/GFP fluorescence intensity ratio. Under control conditions and in cells that were pre-incubated with SB 269970 or MMP-9 inhibitor I, no changes in the mOrange/GFP fluorescence intensity ratio were observed. 5-CT stimulation of neurons isolated from 5-HT7R KO and MMP-9 KO mice did not result in any changes in the mOrange/GFP fluorescence intensity ratio. aaMMP-9 treatment of neurons isolated from 5-HT7R KO mice and MMP-9 KO mice decreased the mOrange/GFP fluorescence intensity ratio.

(B) Quantification of the mOrange/GFP fluorescence intensity ratio 20 min after treatment with 5-CT, SB 269970 + 5-CT, and inhibitor I + 5-CT relative to controls. (5-CT, 0.885 ± 0.027 [n_{cell} = 15]; SB 269970, 1.022 ± 0.024 [n_{cell} = 23]; inhibitor I, 1.001 ± 0.020 [n_{cell} = 14]). 5-CT stimulation of neurons isolated from 5-HT7R KO mice (1.010 ± 0.010, n_{cell} = 13) and MMP-9 KO mice (0.990 ± 0.019, n_{cell} = 17) did not change the mOrange/GFP ratio. After treatment with aaMMP-9, a significant decrease in the mOrange/GFP ratio was observed at 20 min in neurons from both 5-HT7R KO mice (0.856 ± 0.009, n_{cell} = 15) and MMP-9 KO mice (0.846 ± 0.034, n_{cell} = 10). The data are expressed as mean ± SEM (*p < 0.05, **p < 0.01, ***p < 0.001, Student's t test).

Application of 5-CT reduced LTP from 129.6% ± 4.0% to 111.4% ± 4.2% ($p < 0.01$), whereas the effect of 5-CT was completely blocked in the presence of MMP-9 inhibitor I (LTP at 123.8% ± 2.8%; Figures 7A and 7C). Similarly, co-application of the Cdc42 inhibitor ZCL 278 blocked the 5-CT-associated LTP impairment (LTP at 127.8% ± 9.6%; Figures 7B and 7D). These data suggest that 5-HT7R-mediated activation of MMP-9 and Cdc42 are required for the inhibitory effect of 5-CT on LTP.

To examine whether 5-CT mediated LTP reduction correlates with the proteolytic cleavage of endogenous CD44 via MMP-9, hippocampal slices were subjected to western blot analysis after 5-CT stimulation. We separately verified the amount of uncleaved CD44 in the membrane fraction and the amount of 55-kD cleaved CD44 fragment in the extracellular fraction. In slices incubated with 5-CT, we observed accumulation of the 55-kDa cleavage products of CD44 identified with the antibody against the extracellular domain of CD44 in the soluble fraction and a decrease of full-length CD44 in the membrane fraction (Figures 7E and 7F). Pretreatment of the slices with MMP-9 inhibitor I reduced the cleavage of CD44 to baseline level.

DISCUSSION

Since the turn of the millennium, the ECM and extracellular proteases arose as important regulators of synaptic plasticity (Dityatev et al., 2010; Wlodarczyk et al., 2011). We have recently demonstrated that 5-HT7R-mediated signaling also influences neuronal morphology, synaptogenesis, and synaptic plasticity (Kvachnina et al., 2005; Kobe et al., 2012). However, the possible interplay between these signaling pathways has not yet been studied. Here we have shown that the coordinated interplay between 5-HT7R, MMP-9, and CD44 contributes to changes in dendritic spine morphology and affects LTP.

The specific interaction between 5-HT7Rs and CD44 may imply their involvement in the common signaling pathways. 5-HT7Rs are coupled to two different heterotrimeric G-proteins, $G\alpha_S$ and $G\alpha_{12}$, and we have previously shown that the receptor-mediated activation of $G\alpha_{12}$ protein results in the selective activation of the small GTPase Cdc42, which, in turn, promotes the formation of dendritic spines and synaptogenesis (Kvachnina et al., 2005; Kobe et al., 2012). CD44-mediated signaling has also been shown to influence the function of small Rho GTPases in cancer cells (for a review, see Bourguignon, 2008). Both CD44 and Cdc42 are physically linked to IQGAP1 in tumor cells (Bourguignon et al., 2005), and a complex that consists of CD44, Cdc42, and IQGAP1 is able to bind the actin cytoskeleton, thereby regulating actin rearrangement (Briggs and Sacks, 2003). Moreover, CD44-mediated signaling has been shown to stimulate both the Cdc42-CD44 association and PAK1 phosphorylation, leading to the modulation of ovarian tumor cell growth and migration (Bourguignon et al., 2007). A similar interaction between CD44 and Cdc42 might also occur in neurons, in which we observed a high level of expression of CD44 (Figure 4). Functionally, CD44 interaction with 5-HT7Rs can serve as a signal integrator regulating Cdc42 activity toward the modulation of spine morphology. This is supported by the observation that both knockdown of CD44 as well as pharmacological inhibition of Cdc42 result in abolished 5-HT7R-mediated spine elongation (Figure 1).

Using gel zymography, a DQ-gelatin assay (Szepesi et al., 2014), and the MMP-9 biosensor (Stawarski et al., 2014b), we also demonstrated that 5-HT7R-mediated signaling facilitates the enzymatic activity of MMP-9 in primary hippocampal cultures. Concomitantly with measuring gelatinase (MMP-9 and MMP-2) activity, we assayed spine morphology by monitoring the length and head width of individual spines that were targeted by 5-HT7R stimulation in live hippocampal neurons. We found that the changes in gelatinase activity were predominantly localized to elongating spines. This is consistent with a previous observation where MMP-9 activity upon synaptic potentiation localized only to subpopulations of small dendritic spines (Szepesi et al., 2014). Experiments with the MMP-9 biosensor confirmed the increase in MMP-9 activity upon the agonist-dependent activation of 5-HT7Rs. However, the mechanism remains elusive. As mentioned above, 5-HT7Rs are coupled to $G\alpha_S$ and $G\alpha_{12}$. The $G\alpha_{12}$ subunit is known to regulate gene expression by transcriptional activation of distinct transcriptional control elements, such as serum response element (SRE), via activation of small GTPases of the Rho family (Fromm et al., 1997; Mao et al., 1998). We also confirmed that activation of the 5-HT7R/G_{12} signaling pathway results in Rho-dependent activation of SRE (Kvachnina et al., 2005). Functionally, activation of SRE has been shown to be associated with transcription of a variety of immediate-early genes, including the c-*fos* gene (Chai and Tarnawski, 2002), which can bind to the proximal MMP9 promoter region and upregulate the level of MMP-9 enzymatic activity (Kuzniewska et al., 2013).

In addition, MMP-9 can be activated by other mechanisms that might be integrated with the serotonin transmission. It is known that MMP-9 activity can be induced through LTP (Nagy et al., 2006) and that MMP-9 mRNA can undergo quick local translation to dendritic spines, where MMP-9 protein can be released following glutamate stimulation (Dziembowska et al., 2012). This process requires activation of extracellular signal-regulated kinase1/2 (ERK1/2) (Kuzniewska et al., 2013). Thus, 5-HT7R may modulate MMP9 activity through Gs-mediated ERK1/2 signaling. Our study shows a short-term MMP-9 response where the enhanced proteolytic activity is observed 20 min after 5-HT7R stimulation. This indicates that the increase in MMP-9 activity upon receptor stimulation is more likely to be caused by either an increase in local translation or release of previously synthesized MMP-9 rather than transcription regulation, which is a longer process.

MMP-9 was previously shown to bind CD44 and dock close to the membrane in cell lines (Yu and Stamenkovic, 2000; Orgaz et al., 2014). In the present study, we provided direct evidence that CD44 is a target of neuronal MMP-9 in both neuronal cultures and the brain. Using a CD44 shedding reporter, we also demonstrated fast CD44 cleavage upon 5-HT7R stimulation in an MMP-9-dependent manner.

From the functional point of view, CD44 processing is implicated in the modulation of intracellular signaling and morphology. The extracellular cleavage of CD44 results in disruption of cell-matrix interaction, which, in turn, might facilitate the formation of new protrusions. Furthermore, soluble CD44 acts as

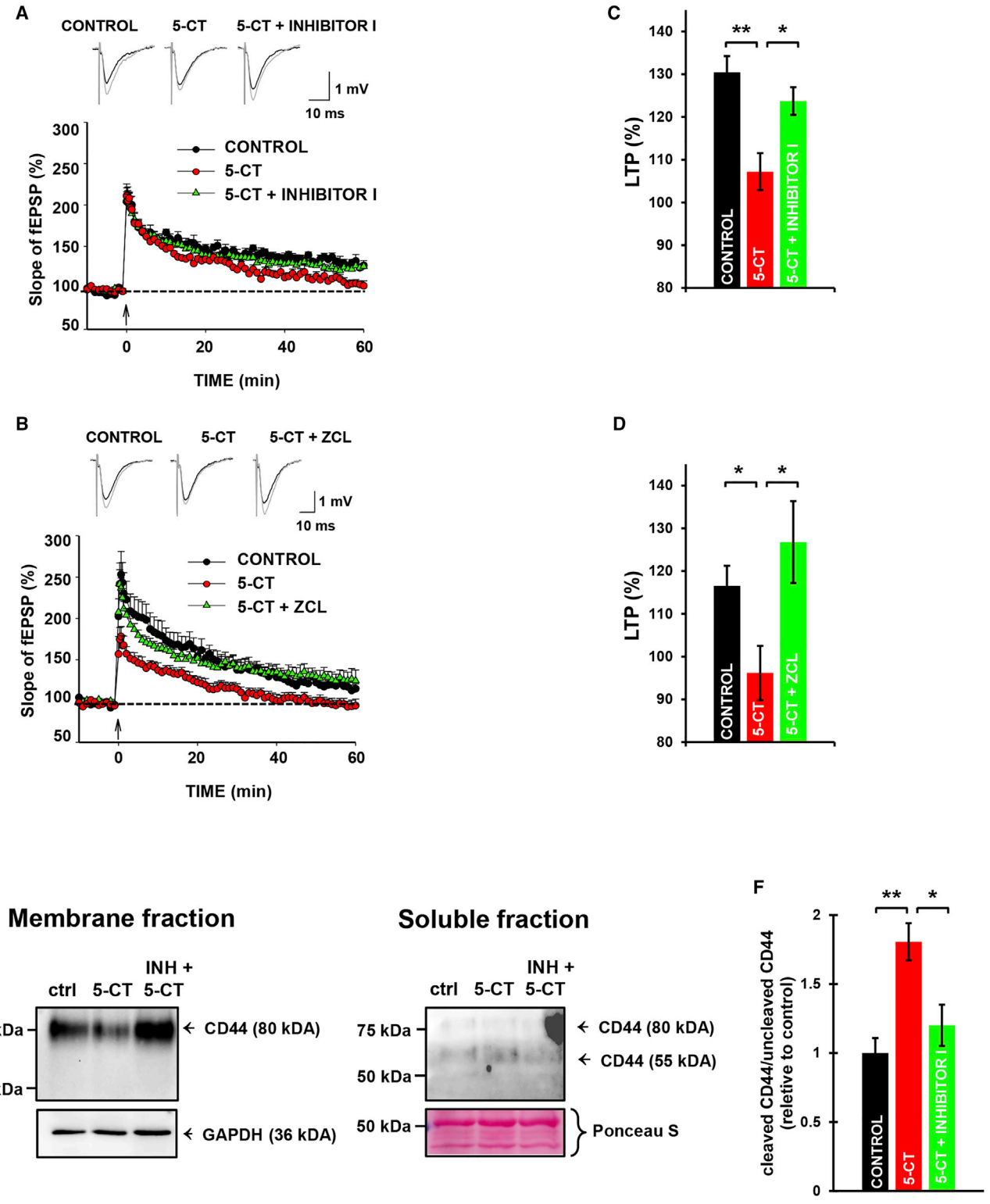

Figure 7. LTP Depends on 5-HT7R/MMP-9/Cdc42 Signaling

(A–D) Application of 5-CT impaired LTP induced by high-frequency stimulation (HFS, indicated by arrows). LTP could be rescued by MMP-9 inhibitor I (A and C) and the Cdc42 inhibitor ZCL 278 (B and D).

(C) Mean ± SEM of LTP levels measured in control slices, slices treated with 5-CT and with Inhibitor I in combination with 5-CT (n = 7, **p < 0.01, *p < 0.05).

(D) Mean ± SEM of LTP levels measured in control slices, slices treated with 5-CT and with Cdc42 inhibitor ZCL in combination with 5-CT (n = 7, *p < 0.05).

(legend continued on next page)

a competitor of endogenous hyaluronan, thus further contributing to detachment of the cell from the ECM (Cichy and Puré, 2003). The intracellular fragment of CD44 has been reported to translocate to the cell nucleus after cleavage and bind to a response element that induces expression of the MMP-9 gene (Miletti-González et al., 2012). Importantly, CD44 and Cdc42 interaction was previously reported (Briggs and Sacks, 2003), implying an influence of CD44 processing on cytoskeleton remodeling and, consequently, dendritic spine morphology. The functional importance of 5-HT7R/MMP-9-mediated processing of CD44 was further supported by the fact that treatment of hippocampal slices with 5-CT resulted in MMP-9-dependent accumulation of 55-kDa cleavage products of CD44, which was accompanied by impaired LTP impairment in the Schaffer collateral synapses (Figure 7). Previous studies revealed that MMP-9 inhibitors impair the late phase of CA1 LTP but have no effects 60 min after induction of LTP (Nagy et al., 2006), whereas this phase of LTP is impaired in MMP-9-overexpressing rats (Magnowska et al., 2016). In line with these data, MMP-9 inhibitor I did not affect CA1 LTP 60 min after induction of LTP but rescued the defect in LTP induced by 5-CT (Figure 7), supporting the view that stimulation of the 5-HT7R activates MMP-9 and that hyperactivity of MMP-9 impairs LTP. In addition, a recent report revealed that postnatal forebrain deletion of Cdc42 leads to impaired LTP in the Schaffer collateral synapses (Kim et al., 2014). Because our data demonstrate rescue of LTP by co-application of 5-CT and the inhibitor of Cdc42 ZCL278, we suggest that there is an optimal range of Cdc42 activity that promotes LTP whereas Cdc42 deficit or hyperactivity impairs it.

5-HT7R KO mice show impaired contextual fear conditioning and reduced CA1 LTP but no significant deficits in motor and spatial learning or cued and operant conditioning (Roberts et al., 2004). A more recent work also demonstrated a normal learning curve in 5-HT7R KO mice and even better spatial memory retention in a Barnes maze (a longer time in the target area 1 month after training) (Sarkisyan and Hedlund, 2009). Thus, the hippocampus-dependent behaviors and CA1 LTP appeared to have bell-shaped dependence on the activity of 5-HT7R, so the lack or excess of activity leads to impaired function. We already made a similar conclusion in respect to Cdc42, the effector downstream of 5-HT7R. Moreover, we hypothesize that morphogenic effects mediated by the 5-HT7Rs, although reducing functional processes underlying re-consolidation of established memories, can be particularly beneficial in the context of reversal learning and cognitive flexibility (Marin and Dityatev, 2017). Indeed, 5-HT7R KO mice are worse in reversal learning in a Barnes maze (Sarkisyan and Hedlund, 2009), and genetic or enzymatic attenuation of the ECM promotes reversal learning in multiple behavioral paradigms (Morellini et al., 2010; Happel et al., 2014). On the other hand, it is known that 5-HT7R KO mice spend less time in rapid eye movement sleep than their WT counterparts (Monti and Jantos, 2014). This may have an effect on memory consolidation and, hence, lead to cognitive impairment independent of the mechanism we have studied. Further behavioral studies are warranted to verify the role of 5-HT7R-controlled proteolysis of CD44 in these aspects of learning and memory (re)consolidation.

Altogether, our data demonstrate that components of the 5-HT7R/Cdc42 signaling pathway, together with CD44 and MMP-9, belong to the same signaling module, which may be responsible for regulating neuronal morphology and plasticity (Figure S8). In this cascade, stimulation of the 5-HT7R results in MMP-9 activation, which, in turn, modulates the activity of CD44 through the proteolytic cleavage of its extracellular domain. This leads to disinhibition of the small GTPase Cdc42, which then becomes more accessible for 5-HT7R-mediated activation. CD44 cleavage also results in partial detachment of the target cell from the ECM, thus facilitating morphological changes mediated by 5-HT7R/Cdc42 signaling. Finally, demonstration of the specific activation of MMP-9 in response to the stimulation of 5-HT7R elucidates a possible role of both MMP-9 and 5-HT7 proteins in establishing pathophysiological conditions, pointing out the 5-HT7R/MMP-9/CD44 signaling module as a target for the treatment of depression and anxiety disorders.

EXPERIMENTAL PROCEDURES

Animals

The experiments were performed with brains from WT, MMP-9-KO (Ducharme et al., 2000), and 5-HT7R KO (Hedlund et al., 2003) mice. All procedures performed on animals were in accordance with the guidelines of the First Warsaw Ethical Committee on Animal Research (permission no. 554/2013).

Cell Culture and Transfection

Mouse N1E-115 neuroblastoma cells from the American Type Culture Collection were grown in DMEM (Gibco) that contained 10% fetal calf serum (FCS, Gibco) and penicillin/streptomycin (100 U/mL, Gibco) at 37°C under 5% CO_2. Transient transfection was performed with Lipofectamine 2000 (Invitrogen) according to the manufacturer's instructions.

Preparation, Transfection, and Treatment of Hippocampal Neurons

Mouse primary hippocampal neurons were prepared as described previously (Kobe et al., 2012). Rat hippocampal organotypic slices were prepared according to Stoppini et al. (1991). See the Supplemental Experimental Procedures for details and treatments.

Immunofluorescence

For experimental details and a list of antibodies and usage, see the Supplemental Experimental Procedures.

Live-Cell Imaging

Prior to imaging, the cells were mounted in an acquisition chamber. The osmolality of the buffer was adjusted to the osmolality (± 15 mOsm) of the maintenance medium. Images were acquired using a Zeiss LSM 780 confocal microscope with a long distance (LD) C-Apochromat 40×/1.1 W Korr M27 water immersion objective. For experimental details, see the Supplemental Experimental Procedures.

Values obtained in (C) and (D) were measured as average slope of EPSPs recorded 50–60 min after HFS relative to the average slope of baseline fEPSPs.
(E) Western blot analysis of CD44 cleavage in membrane and soluble fractions in control and 5-CT- and 5-CT + inhibitor I-treated hippocampal slices. Treatment with 5-CT results in an increased amount of 55-kDa cleavage CD44 fragment in soluble fraction and a decrease in full-length CD44 in the membrane fraction.
(F) Quantification of the ratio of 55-kDa CD44 in the soluble fraction over full-length CD44 in the membrane fraction in control and 5-CT- and 5-CT + inhibitor I-treated hippocampal slices. Glyceraldehyde-3-phosphate dehydrogenase (GAPDH) was used as a calibrator.

Biochemical Methods

Standard methodologies for coIP, western blotting, and gel zymography were used. For experimental details and a list of antibodies and usage, see the Supplemental Experimental Procedures.

Electrophysiology

For experimental details, see the Supplemental Experimental Procedures.

Two-Photon Excitation Imaging and Uncaging

For experimental details, see the Supplemental Experimental Procedures.

Statistical Analysis

For details, see the Supplemental Experimental Procedures.

SUPPLEMENTAL INFORMATION

Supplemental Information includes Supplemental Experimental Procedures and eight figures and can be found with this article online at http://dx.doi.org/10.1016/j.celrep.2017.05.023.

AUTHOR CONTRIBUTIONS

E.P., J.W., G.W., and J.D. conceived the study. M. Bijata, A.D., J.W., E.P., and D.A.R. designed the experiments. M. Bijata, J.L., P.M., D.G., J.S., and K.B. performed the experiments. M. Bijata, J.L., M. Butzlaff, and D.A.R. analyzed the data. J.W., P.M., A.D., E.P., and M.S. contributed reagents, materials, and analysis tools. A.D., M. Bijata, J.W., J.L., E.P., and D.A.R. wrote the paper.

ACKNOWLEDGMENTS

This work was supported by the National Science Centre (grant UMO-2012/06/M/NZ3/00163), the National Centre for Research and Development (grant TANGO1/269352/NCBR/2015), Deutsche Forschungsgemeinschaft (grant PO732, excellence cluster REBIRTH), TargetECM/BMBF funding for the TargetECM project (01EW1308B to E.P. and A.D.), and BMBF funding for the SmartAge project (01GQ1420D to E.P.). We would like to thank Dr. Erwin Neher for critical discussions.

Received: November 8, 2016
Revised: April 3, 2017
Accepted: May 4, 2017
Published: May 30, 2017

REFERENCES

Bajor, M., Michaluk, P., Gulyassy, P., Kekesi, A.K., Juhasz, G., and Kaczmarek, L. (2012). Synaptic cell adhesion molecule-2 and collapsin response mediator protein-2 are novel members of the matrix metalloproteinase-9 degradome. J. Neurochem. *122*, 775–788.

Boddum, K., Jensen, T.P., Magloire, V., Kristiansen, U., Rusakov, D.A., Pavlov, I., and Walker, M.C. (2016). Astrocytic GABA transporter activity modulates excitatory neurotransmission. Nat. Commun. *7*, 13572.

Bourguignon, L.Y.W. (2008). Hyaluronan-mediated CD44 activation of RhoGTPase signaling and cytoskeleton function promotes tumor progression. Semin. Cancer Biol. *18*, 251–259.

Bourguignon, L.Y.W., Gilad, E., Rothman, K., and Peyrollier, K. (2005). Hyaluronan-CD44 interaction with IQGAP1 promotes Cdc42 and ERK signaling, leading to actin binding, Elk-1/estrogen receptor transcriptional activation, and ovarian cancer progression. J. Biol. Chem. *280*, 11961–11972.

Bourguignon, L.Y.W., Gilad, E., and Peyrollier, K. (2007). Heregulin-mediated ErbB2-ERK signaling activates hyaluronan synthases leading to CD44-dependent ovarian tumor cell growth and migration. J. Biol. Chem. *282*, 19426–19441.

Briggs, M.W., and Sacks, D.B. (2003). IQGAP proteins are integral components of cytoskeletal regulation. EMBO Rep. *4*, 571–574.

Brown, M.D., Cornejo, B.J., Kuhn, T.B., and Bamburg, J.R. (2000). Cdc42 stimulates neurite outgrowth and formation of growth cone filopodia and lamellipodia. J. Neurobiol. *43*, 352–364.

Carter, W.G., and Wayner, E.A. (1988). Characterization of the class III collagen receptor, a phosphorylated, transmembrane glycoprotein expressed in nucleated human cells. J. Biol. Chem. *263*, 4193–4201.

Chai, J., and Tarnawski, A.S. (2002). Serum response factor: discovery, biochemistry, biological roles and implications for tissue injury healing. J. Physiol. Pharmacol. *53*, 147–157.

Cichy, J., and Puré, E. (2003). The liberation of CD44. J. Cell Biol. *161*, 839–843.

Dityatev, A., Schachner, M., and Sonderegger, P. (2010). The dual role of the extracellular matrix in synaptic plasticity and homeostasis. Nat. Rev. Neurosci. *11*, 735–746.

Dorsch, S., Klotz, K.-N., Engelhardt, S., Lohse, M.J., and Bünemann, M. (2009). Analysis of receptor oligomerization by FRAP microscopy. Nat. Methods *6*, 225–230.

Ducharme, A., Frantz, S., Aikawa, M., Rabkin, E., Lindsey, M., Rohde, L.E., Schoen, F.J., Kelly, R.A., Werb, Z., Libby, P., and Lee, R.T. (2000). Targeted deletion of matrix metalloproteinase-9 attenuates left ventricular enlargement and collagen accumulation after experimental myocardial infarction. J. Clin. Invest. *106*, 55–62.

Duterme, C., Mertens-Strijthagen, J., Tammi, M., and Flamion, B. (2009). Two novel functions of hyaluronidase-2 (Hyal2) are formation of the glycocalyx and control of CD44-ERM interactions. J. Biol. Chem. *284*, 33495–33508.

Dziembowska, M., Milek, J., Janusz, A., Rejmak, E., Romanowska, E., Gorkiewicz, T., Tiron, A., Bramham, C.R., and Kaczmarek, L. (2012). Activity-dependent local translation of matrix metalloproteinase-9. J. Neurosci. *32*, 14538–14547.

Ethell, I.M., and Ethell, D.W. (2007). Matrix metalloproteinases in brain development and remodeling: synaptic functions and targets. J. Neurosci. Res. *85*, 2813–2823.

Friesland, A., Zhao, Y., Chen, Y.-H., Wang, L., Zhou, H., and Lu, Q. (2013). Small molecule targeting Cdc42-intersectin interaction disrupts Golgi organization and suppresses cell motility. Proc. Natl. Acad. Sci. USA *110*, 1261–1266.

Fromm, C., Coso, O.A., Montaner, S., Xu, N., and Gutkind, J.S. (1997). The small GTP-binding protein Rho links G protein-coupled receptors and Galpha12 to the serum response element and to cellular transformation. Proc. Natl. Acad. Sci. USA *94*, 10098–10103.

Happel, M.F., Niekisch, H., Castiblanco Rivera, L.L., Ohl, F.W., Deliano, M., and Frischknecht, R. (2014). Enhanced cognitive flexibility in reversal learning induced by removal of the extracellular matrix in auditory cortex. Proc. Natl. Acad. Sci. USA *111*, 2800–2805.

Harrison, C., and van der Graaf, P.H. (2006). Current methods used to investigate G protein coupled receptor oligomerisation. J. Pharmacol. Toxicol. Methods *54*, 26–35.

Hedlund, P.B. (2009). The 5-HT7 receptor and disorders of the nervous system: an overview. Psychopharmacology (Berl.) *206*, 345–354.

Hedlund, P.B., Danielson, P.E., Thomas, E.A., Slanina, K., Carson, M.J., and Sutcliffe, J.G. (2003). No hypothermic response to serotonin in 5-HT7 receptor knockout mice. Proc. Natl. Acad. Sci. USA *100*, 1375–1380.

Huntley, G.W. (2012). Synaptic circuit remodelling by matrix metalloproteinases in health and disease. Nat. Rev. Neurosci. *13*, 743–757.

James, J.R., Oliveira, M.I., Carmo, A.M., Iaboni, A., and Davis, S.J. (2006). A rigorous experimental framework for detecting protein oligomerization using bioluminescence resonance energy transfer. Nat. Methods *3*, 1001–1006.

Jontes, J.D., and Smith, S.J. (2000). Filopodia, spines, and the generation of synaptic diversity. Neuron *27*, 11–14.

Kalomiris, E.L., and Bourguignon, L.Y. (1988). Mouse T lymphoma cells contain a transmembrane glycoprotein (GP85) that binds ankyrin. J. Cell Biol. *106*, 319–327.

Kim, I.H., Wang, H., Soderling, S.H., and Yasuda, R. (2014). Loss of Cdc42 leads to defects in synaptic plasticity and remote memory recall. eLife *3*.

Kobe, F., Guseva, D., Jensen, T.P., Wirth, A., Renner, U., Hess, D., Müller, M., Medrihan, L., Zhang, W., Zhang, M., et al. (2012). 5-HT7R/G12 signaling regulates neuronal morphology and function in an age-dependent manner. J. Neurosci. *32*, 2915–2930.

Kochlamazashvili, G., Henneberger, C., Bukalo, O., Dvoretskova, E., Senkov, O., Lievens, P.M.-J., Westenbroek, R., Engel, A.K., Catterall, W.A., Rusakov, D.A., et al. (2010). The extracellular matrix molecule hyaluronic acid regulates hippocampal synaptic plasticity by modulating postsynaptic L-type Ca(2+) channels. Neuron *67*, 116–128.

Kuzniewska, B., Rejmak, E., Malik, A.R., Jaworski, J., Kaczmarek, L., and Kalita, K. (2013). Brain-derived neurotrophic factor induces matrix metalloproteinase 9 expression in neurons via the serum response factor/c-Fos pathway. Mol. Cell. Biol. *33*, 2149–2162.

Kvachnina, E., Liu, G., Dityatev, A., Renner, U., Dumuis, A., Richter, D.W., Dityateva, G., Schachner, M., Voyno-Yasenetskaya, T.A., and Ponimaskin, E.G. (2005). 5-HT7 receptor is coupled to G alpha subunits of heterotrimeric G12-protein to regulate gene transcription and neuronal morphology. J. Neurosci. *25*, 7821–7830.

Magnowska, M., Gorkiewicz, T., Suska, A., Wawrzyniak, M., Rutkowska-Wlodarczyk, I., Kaczmarek, L., and Wlodarczyk, J. (2016). Transient ECM protease activity promotes synaptic plasticity. Sci. Rep. *6*, 27757.

Mao, J., Yuan, H., Xie, W., and Wu, D. (1998). Guanine nucleotide exchange factor GEF115 specifically mediates activation of Rho and serum response factor by the G protein alpha subunit Galpha13. Proc. Natl. Acad. Sci. USA *95*, 12973–12976.

Marin, P., and Dityatev, A. (2017). 5-HT7R shapes spinogenesis in cortical and striatal neurons. J. Neurochem. http://dx.doi.org/10.1111/jnc.13981.

Marrero-Diaz, R., Bravo-Cordero, J.J., Megías, D., García, M.A., Bartolomé, R.A., Teixido, J., and Montoya, M.C. (2009). Polarized MT1-MMP-CD44 interaction and CD44 cleavage during cell retraction reveal an essential role for MT1-MMP in CD44-mediated invasion. Cell Motil. Cytoskeleton *66*, 48–61.

Matthys, A., Haegeman, G., Van Craenenbroeck, K., and Vanhoenacker, P. (2011). Role of the 5-HT7 receptor in the central nervous system: from current status to future perspectives. Mol. Neurobiol. *43*, 228–253.

Michaluk, P., Kolodziej, L., Mioduszewska, B., Wilczynski, G.M., Dzwonek, J., Jaworski, J., Gorecki, D.C., Ottersen, O.P., and Kaczmarek, L. (2007). Beta-dystroglycan as a target for MMP-9, in response to enhanced neuronal activity. J. Biol. Chem. *282*, 16036–16041.

Michaluk, P., Wawrzyniak, M., Alot, P., Szczot, M., Wyrembek, P., Mercik, K., Medvedev, N., Wilczek, E., De Roo, M., Zuschratter, W., et al. (2011). Influence of matrix metalloproteinase MMP-9 on dendritic spine morphology. J. Cell Sci. *124*, 3369–3380.

Miletti-González, K.E., Murphy, K., Kumaran, M.N., Ravindranath, A.K., Wernyj, R.P., Kaur, S., Miles, G.D., Lim, E., Chan, R., Chekmareva, M., et al. (2012). Identification of function for CD44 intracytoplasmic domain (CD44-ICD): modulation of matrix metalloproteinase 9 (MMP-9) transcription via novel promoter response element. J. Biol. Chem. *287*, 18995–19007.

Monti, J.M., and Jantos, H. (2014). The role of serotonin 5-HT7 receptor in regulating sleep and wakefulness. Rev. Neurosci. *25*, 429–437.

Morellini, F., Sivukhina, E., Stoenica, L., Oulianova, E., Bukalo, O., Jakovcevski, I., Dityatev, A., Irintchev, A., and Schachner, M. (2010). Improved reversal learning and working memory and enhanced reactivity to novelty in mice with enhanced GABAergic innervation in the dentate gyrus. Cereb. Cortex *20*, 2712–2727.

Nagy, V., Bozdagi, O., Matynia, A., Balcerzyk, M., Okulski, P., Dzwonek, J., Costa, R.M., Silva, A.J., Kaczmarek, L., and Huntley, G.W. (2006). Matrix metalloproteinase-9 is required for hippocampal late-phase long-term potentiation and memory. J. Neurosci. *26*, 1923–1934.

Newey, S.E., Velamoor, V., Govek, E.-E., and Van Aelst, L. (2005). Rho GTPases, dendritic structure, and mental retardation. J. Neurobiol. *64*, 58–74.

Norum, J.H., Hart, K., and Levy, F.O. (2003). Ras-dependent ERK activation by the human G(s)-coupled serotonin receptors 5-HT4(b) and 5-HT7(a). J. Biol. Chem. *278*, 3098–3104.

Okamoto, I., Kawano, Y., Tsuiki, H., Sasaki, J., Nakao, M., Matsumoto, M., Suga, M., Ando, M., Nakajima, M., and Saya, H. (1999). CD44 cleavage induced by a membrane-associated metalloprotease plays a critical role in tumor cell migration. Oncogene *18*, 1435–1446.

Orgaz, J.L., Pandya, P., Dalmeida, R., Karagiannis, P., Sanchez-Laorden, B., Viros, A., Albrengues, J., Nestle, F.O., Ridley, A.J., Gaggioli, C., et al. (2014). Diverse matrix metalloproteinase functions regulate cancer amoeboid migration. Nat. Commun. *5*, 4255.

Roberts, A.J., Krucker, T., Levy, C.L., Slanina, K.A., Sutcliffe, J.G., and Hedlund, P.B. (2004). Mice lacking 5-HT receptors show specific impairments in contextual learning. Eur. J. Neurosci. *19*, 1913–1922.

Rusakov, D.A., and Fine, A. (2003). Extracellular Ca2+ depletion contributes to fast activity-dependent modulation of synaptic transmission in the brain. Neuron *37*, 287–297.

Rybakowski, J.K., Remlinger-Molenda, A., Czech-Kucharska, A., Wojcicka, M., Michalak, M., and Losy, J. (2013). Increased serum matrix metalloproteinase-9 (MMP-9) levels in young patients during bipolar depression. J. Affect. Disord. *146*, 286–289.

Sala, C., and Segal, M. (2014). Dendritic spines: the locus of structural and functional plasticity. Physiol. Rev. *94*, 141–188.

Sarkisyan, G., and Hedlund, P.B. (2009). The 5-HT7 receptor is involved in allocentric spatial memory information processing. Behav. Brain Res. *202*, 26–31.

Skupien, A., Konopka, A., Trzaskoma, P., Labus, J., Gorlewicz, A., Swiech, L., Babraj, M., Dolezyczek, H., Figiel, I., Ponimaskin, E., et al. (2014). CD44 regulates dendrite morphogenesis through Src tyrosine kinase-dependent positioning of the Golgi. J. Cell Sci. *127*, 5038–5051.

Stawarski, M., Stefaniuk, M., and Wlodarczyk, J. (2014a). Matrix metalloproteinase-9 involvement in the structural plasticity of dendritic spines. Front. Neuroanat. *8*, 68.

Stawarski, M., Rutkowska-Wlodarczyk, I., Zeug, A., Bijata, M., Madej, H., Kaczmarek, L., and Wlodarczyk, J. (2014b). Genetically encoded FRET-based biosensor for imaging MMP-9 activity. Biomaterials *35*, 1402–1410.

Stoppini, L., Buchs, P.A., and Muller, D. (1991). A simple method for organotypic cultures of nervous tissue. J. Neurosci. Methods *37*, 173–182.

Szepesi, Z., Bijata, M., Ruszczycki, B., Kaczmarek, L., and Wlodarczyk, J. (2013). Matrix metalloproteinases regulate the formation of dendritic spine head protrusions during chemically induced long-term potentiation. PLoS ONE *8*, e63314.

Szepesi, Z., Hosy, E., Ruszczycki, B., Bijata, M., Pyskaty, M., Bikbaev, A., Heine, M., Choquet, D., Kaczmarek, L., and Wlodarczyk, J. (2014). Synaptically released matrix metalloproteinase activity in control of structural plasticity and the cell surface distribution of GluA1-AMPA receptors. PLoS ONE *9*, e98274.

Udo, H., Jin, I., Kim, J.-H., Li, H.-L., Youn, T., Hawkins, R.D., Kandel, E.R., and Bailey, C.H. (2005). Serotonin-induced regulation of the actin network for learning-related synaptic growth requires Cdc42, N-WASP, and PAK in Aplysia sensory neurons. Neuron *45*, 887–901.

Vandooren, J., Geurts, N., Martens, E., Van den Steen, P.E., and Opdenakker, G. (2013). Zymography methods for visualizing hydrolytic enzymes. Nat. Methods *10*, 211–220.

Wang, X.B., Bozdagi, O., Nikitczuk, J.S., Zhai, Z.W., Zhou, Q., and Huntley, G.W. (2008). Extracellular proteolysis by matrix metalloproteinase-9 drives dendritic spine enlargement and long-term potentiation coordinately. Proc. Natl. Acad. Sci. USA *105*, 19520–19525.

Weber, G.F., Ashkar, S., Glimcher, M.J., and Cantor, H. (1996). Receptor-ligand interaction between CD44 and osteopontin (Eta-1). Science *271*, 509–512.

Wlodarczyk, J., Woehler, A., Kobe, F., Ponimaskin, E., Zeug, A., and Neher, E. (2008). Analysis of FRET signals in the presence of free donors and acceptors. Biophys. J. *94*, 986–1000.

Wlodarczyk, J., Mukhina, I., Kaczmarek, L., and Dityatev, A. (2011). Extracellular matrix molecules, their receptors, and secreted proteases in synaptic plasticity. Dev. Neurobiol. *71*, 1040–1053.

Yu, Q., and Stamenkovic, I. (2000). Cell surface-localized matrix metalloproteinase-9 proteolytically activates TGF-β and promotes tumor invasion and angiogenesis. Genes Dev. *14*, 163–176.